



## Review

## A survey of tellurium-centered secondary-bonding supramolecular synthons

Anthony F. Cozzolino, Philip J.W. Elder, Ignacio Vargas-Baca\*

Department of Chemistry and Chemical Biology, McMaster University, 1280 Main Street West, Hamilton, Ontario, Canada L8S 4M1

## Contents

1. Introduction .....	1426
2. Search criteria and selection of Te–D contacts .....	1428
3. Tellurium-centered supramolecular synthons .....	1428
3.1. Classification and notation .....	1428
3.2. The supramolecular synthon with a single point of attachment: [Te D] .....	1429
3.3. Supramolecular synthons with two points of attachment .....	1430
3.3.1. [Te D–m–D] .....	1430
3.3.2. [Te–m–Te D] .....	1433
3.3.3. [Te–m–D] <sub>2</sub> .....	1434
3.4. Supramolecular synthons with four points of attachment .....	1436
3.4.1. [Te–m–Te–m–D] <sub>2</sub> .....	1436
3.4.2. [Te–m–Te–m–D–m–D] <sub>2</sub> .....	1436
3.4.3. [Te–m–D–m–D] <sub>2</sub> or [D–m–Te–m–D] <sub>2</sub> .....	1437
4. Conclusions .....	1437
References .....	1437

## ARTICLE INFO

## Article history:

Received 3 September 2010

Accepted 15 December 2010

Available online 23 December 2010

## Keywords:

Supramolecular chemistry

Self-assembly

Tellurium

Organochalcogen chemistry

Secondary bonding

Intermolecular interactions

## ABSTRACT

The crystal structures of tellurium compounds frequently display intermolecular contacts between the chalcogen and atoms possessing lone pairs of electrons. Analysis of the data deposited in the Cambridge crystallographic database shows that the shortest secondary bonding interactions (SBIs) are formed when oxygen, nitrogen or chlorine are the donor atoms for SBIs. In addition, these SBIs are shortest when they occur opposite to a bond between tellurium and oxygen, nitrogen, fluorine, chlorine or the nitrile functional group. The structural motifs assembled in these systems fall within eight general categories, from single to multiple bonded supramolecular synthons. The use of multiple points of attachment between molecules leads, in principle, to stronger and more directional supramolecular synthons. The overall structures assembled by the most important tellurium-based supramolecular synthons and prospects for their application in crystal engineering are discussed.

© 2010 Elsevier B.V. All rights reserved.

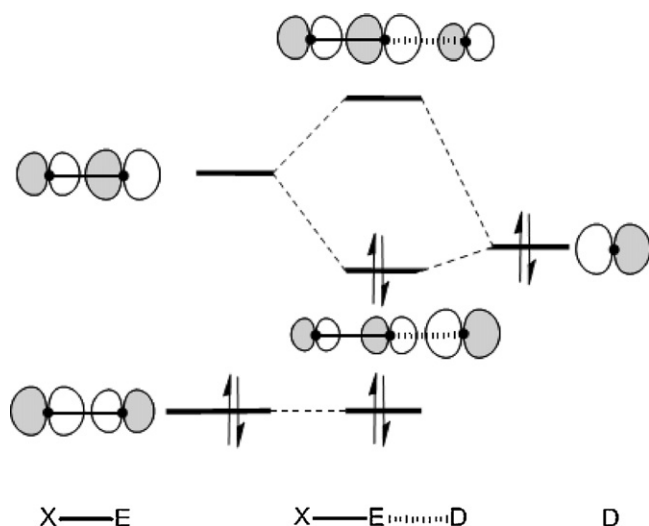
## 1. Introduction

In view of the wide extent of the achievements attained in over 40 years of research in supramolecular chemistry and its subfields (e.g. self-assembly, host–guest chemistry, solid-state inclusion chemistry, crystal engineering, supramolecular machines/devices and soft/smart materials), it is remarkable that most large, complex and sometimes functional *polymolecular entities* [1] have been obtained with the use of just a few types of supramolecular interactions: hydrogen bonding, the coordination of metal ions and, to a lesser extent,  $\pi$ -stacking and hydrophobic effects.

Under the premise that different interactions would lead to distinct architectures and/or elicit unique properties, other interactions have stimulated interest as alternative tools for the formation of supramolecular assemblies. For example, *aurophilic* (or more generally *metalophilic*) interactions between  $d^{10}$  metal ions continue to attract interest because of the intriguing structures and photophysical properties of the compounds that feature them [2]. Such contacts are stabilized by relativistic effects and belong to the broad category of *closed-shell* interactions [3], meaning that the participating atoms had already satisfied their valences and – based on the simple arguments of Lewis bonding theory – were not expected to require more bonding electrons and/or form additional bonds.

Closed-shell interactions are a pervasive feature in structural main-group chemistry [4]; crystallographic determinations often reveal short distances between a heavy p-block element and one or

\* Corresponding author. Tel.: +1 905 525 9140x23497; fax: +1 905 522 2509.  
E-mail address: [vargas@chemistry.mcmaster.ca](mailto:vargas@chemistry.mcmaster.ca) (I. Vargas-Baca).



**Fig. 1.** Molecular orbital interaction for E–D secondary bonding. For simplicity, only p atomic orbitals are considered.

more atoms which typically possess lone pairs of electrons. Heavy main-group elements are of course able to “expand their valence shell” forming *hypervalent bonds* that are accurately described by multicenter orbital interactions but the distances in closed-shell interactions are much longer than the typical hypervalent single bond and yet they are so much shorter than the sum of the corresponding van der Waals radii that they cannot be dismissed as “non-bonded contacts” or “packing accidents” stabilized only by “van der Waals forces”.<sup>1</sup> Over time this phenomenon has received attention under several labels including: soft–soft interactions [5], closed-shell interactions [3], nonbonding interactions [6],  $\sigma$ -hole interactions [7], semibonding interactions [8], halogen bonds [9], noncovalent interactions [10] and weakly bonding interactions [11–13]. Arguably the most appropriate name, *secondary bonding interaction* (SBI), was proposed in the 1970s by Alcock [14] making distinction from the Lewis and hypervalent *primary* bonds. His concept was based on crystallographic data, including not only distances but angles as well. Considering that typically the secondary bond axis is nearly collinear with a (primary) bond between the central heavy atom (E) and a more electronegative atom (X), Alcock realized that such interactions are stabilized by electrostatic and covalent contributions. The former arises from local partial charges and the latter consists of the donation of electrons into the  $\sigma^*$  molecular orbital corresponding to the primary E–X bond (Fig. 1). The fundamentals of this model derived from empirical observation have been validated by modern quantum mechanical methods [15,16] but a complete bonding description does require the inclusion of all orbital, electrostatic and dispersion contributions [6]. While mixing of occupied and unoccupied orbitals corresponds to the donor–acceptor character of the interaction and confers directionality to the SBI, an unavoidable destabilizing contribution (the Pauli repulsion) results from the mixing of all-occupied orbitals. In certain cases, the electrostatic contribution could add to the direc-

tional nature of the SBI [7,9,17]. The dispersion force is always attractive and arises from the instantaneous correlation of electrons in the interacting atoms. The strength of the dispersion force increases as the electron clouds become more polarizable; it is therefore more important for systems with the heaviest elements [18,19]. Although SBIs are not fundamentally different from “regular” hypervalent bonds – and in certain instances can approach their strength [56] – it is convenient to distinguish SBIs as the interactions or bonds which can be manipulated for the purposes of supramolecular synthesis.

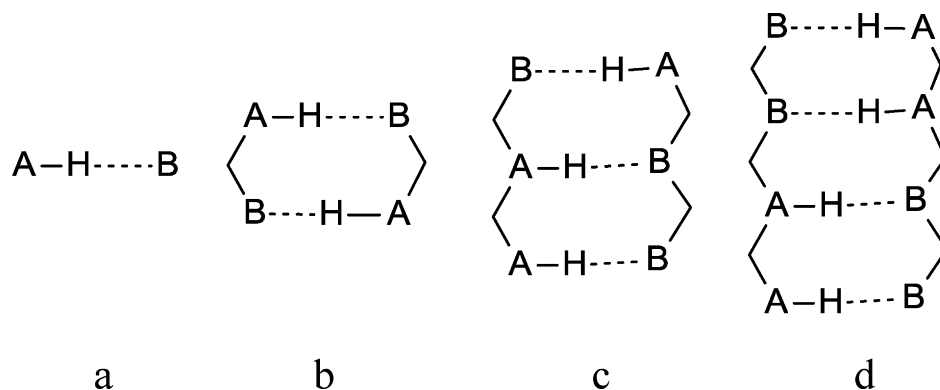
Compared to other supramolecular interactions, there have been rather few attempts to systematically use SBIs as design elements in supramolecular chemistry. Notwithstanding, some noteworthy cases illustrate the potential of main-group SBIs in this context: pnictogen-centered SBIs [20] can link ribbon polymers [21]; chalcogen–chalcogen contacts [22] assemble supramolecular tubes [6,23–25]; and applications of halogen SBIs have been demonstrated in the design of noncentrosymmetric lattices capable of second harmonic generation (SHG) [26], the resolution of a racemic perfluoroalkyl bromide [27], the separation of mixtures of diiodoperfluoroalkanes [28], and the organization of 1-dimensional molecular magnets with attenuation of antiferromagnetic coupling [29]. Making an analogy to hydrogen bonding, Starbuck and Orpen [30] noted that the rational design of SBI supramolecular systems would greatly benefit from the application of Desiraju’s concept of supramolecular synthon: “a structural unit within a supermolecule which can be formed and/or assembled by known or conceivable synthetic operations involving intermolecular interactions” [30]. Scheme 1 depicts some important examples of dimeric supramolecular synthons that are based on hydrogen bonding. The key to an efficient application of main-group SBIs in supramolecular chemistry would be the identification of the most efficient supramolecular synthons, i.e. those which are:

- Strong enough to hold the building blocks in place.
- Directional to guide the formation of the supramolecular structure.
- Reversible in order to allow error self-correction.
- Synthetically accessible by methods applicable to a wide variety of derivatives.

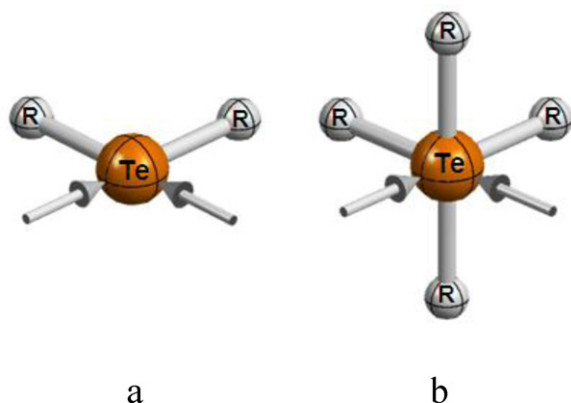
The case of hydrogen bonding does illustrate how supramolecular synthons with multiple points of attachment achieve great stability and directionality, as in the synthons that are formed by the pairing of bases in nucleic acids (Scheme 1b and c) and a motif which is so strong that it generates true supramolecular polymers (Scheme 1d) [31].

We have been interested in the chalcogens (S, Se, and Te) as SBI centers because their VSEPR geometries in oxidation states II and IV typically have two positions available for the formation of SBIs (Fig. 2); such a geometric attribute encourages chelation and/or the formation of planar supramolecular synthons. Because of the antibonding character of the electron-acceptor orbitals, the heaviest member of the family, tellurium, makes the strongest SBIs. Tellurium is synthetically versatile as it makes stable bonds with most main-group elements [32]. The ability of some tellurium compounds to form adducts with organic Lewis bases has long been recognized [33] and in fact, Haiduc and Zukerman-Schpector [22,34] have reviewed a number of supramolecular structures assembled by tellurium-centered SBIs. The present overview of the data deposited in the Cambridge Crystallographic Database (CSD, version 5.31, Nov. 2009 with 490,902 entries) [35] is intended to extend those earlier findings with a comparison of the relative strengths of tellurium-centered SBIs and the identification of their most frequent and strongest

<sup>1</sup> Considering its origin in modelling gas behaviour, the term “van der Waals forces” is in principle applicable to *any* intermolecular interactions but it is most frequently used to describe those arising from dipole–dipole, dipole-induced dipole or dispersion forces. On the other hand, the van der Waals radius is an arbitrary cutoff distance, beyond which intermolecular contacts are regarded as the result of those weak interactions only. However, such interpretation is in conflict with the asymptotic radial decay of electron density from the atomic nucleus; in other words, there is always some degree of orbital interaction between the molecules.



**Scheme 1.** H-bonded supramolecular synthons. A and B denote acidic (H donor) and basic (H acceptor) sites.



**Fig. 2.** Idealized VSEPR geometries for tellurium in the (a) II and (b) IV oxidation states. The arrows denote the positions preferred by secondary bonding interactions.

supramolecular synthons; it constitutes an attempt to assess the viability of applying such structural motifs in supramolecular chemistry.

## 2. Search criteria and selection of Te–D contacts

The packing and organization motifs of all tellurium containing structures in the database could, in principle, be analyzed but to simplify their classification this survey was limited to systems that possess the strongest SBIs, as estimated from the contact distances. Although the actual strength of an intermolecular interaction cannot be accurately established from structural data alone, the interatomic distances can be used as a semiquantitative indicator of their relative strength: SBIs with distances close to the sum of van der Waals radii would be primarily stabilized by dispersion, while shorter SBIs would also have important covalent and electrostatic components. In order to discriminate the weakest interactions, our analysis is restricted to those cases in which the SBI falls within a cutoff distance equal to 93% of the sum of Bondi's [36] van der Waals radii. This limit was chosen based on recent work by Rowland and Taylor [37] as well as Dance [38] who noted that interatomic contacts (for any pair of elements) with a primarily dispersive origin follow a normal distribution centered at ca. 10% above the sum of corresponding van der Waals radii. In other words, we have excluded those distances which fall within twice the standard deviation of the distribution of dispersive contacts.

As defined in the CSD [35], 1241 structures (40% out of a total of 3133 Te-containing compounds) contain short intermolecular contacts (those which are below 1.1 times the sum of van der Waals

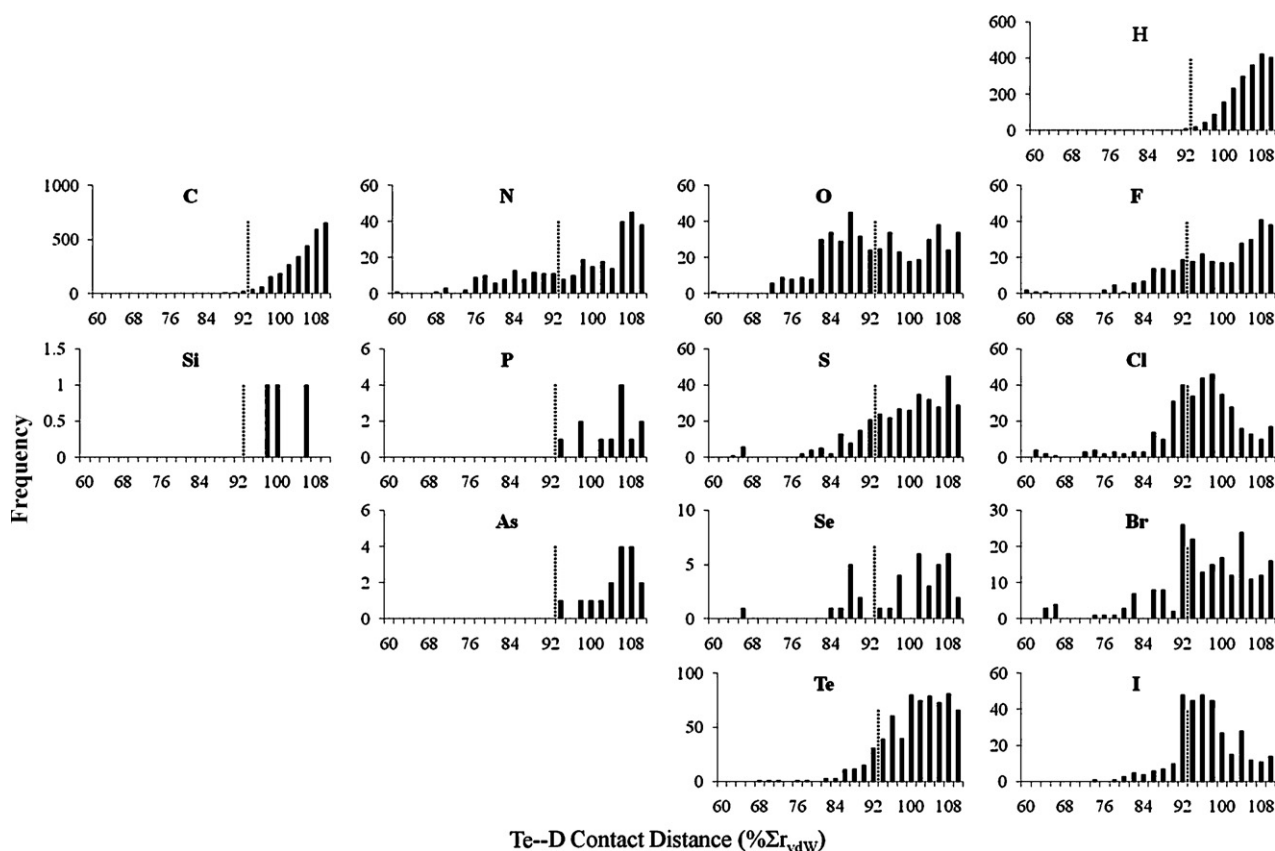
radii) between Te and H, C, Si or D where D is N, O, F, P, S, Cl, As, Se, Br, Sb, Te, or I (excluding cases that contain metals and/or molecular ions). The corresponding Te–D histograms (for 2719 distances in total) are displayed in Fig. 3. The figure also features histograms for 2057 Te–H, and 2797 Te–C short contacts; although there are only 3 Te–Si contacts the data is included for comparison. The histograms illustrate that when the atom in contact with Te does not have available lone pairs (e.g. Si, C and H) the frequency of contacts increases with interatomic distance. This is characteristic of a random spatial distribution of contacts and indicates that these contacts would only be stabilized by dispersion [37]. In contrast, the histograms for Te contacts with the most electronegative atoms have the largest proportion of very short distances. These short interactions are the most likely to correspond to strong Te-containing supramolecular synthons. Te contacts with P and As appear to be rather weak as most appear beyond 93% of the sum of van der Waals radii.

## 3. Tellurium-centered supramolecular synthons

### 3.1. Classification and notation

In order to facilitate the classification, comparison, and subsequent discussion of supramolecular synthons that are assembled from dissimilar building blocks, the following shorthand notation is used: the label  $[E-m-D]_n$  denotes in square brackets the *molecular fragments* of the building blocks that comprise the supramolecular synthon. E and D are the elements that engage in SBIs; in this review E is always Te. A dash indicates a covalent link between E and D while no dash implies that the atoms belong to different molecules. For simplicity, the bridging atoms linking E and D are not explicitly identified, only how many (*m*). The subscript *n* is the number of times the fragments are repeated in the structure of the supramolecular synthon, or in other words how many building blocks assemble it. The subscript is obviated when *n* = 1. This notation is applied in Fig. 4 to the supramolecular synthons assembled by short Te–D SBIs which were most frequently found in the database. The first example  $[Te-m-D]$  corresponds to an intramolecular SBI. Such virtual rings are a frequent feature in the structures of compounds of p-block elements [12,39]; however, the intramolecular phenomenon is outside the scope of this review.

An alternative notation based on the application of graph set theory (GST) is applicable to supramolecular systems assembled by SBIs. GST constitutes a powerful method for the systematic analysis and description of a crystal structure in terms of all intermolecular interactions [49,50]. However, GST notation makes no distinction of the nature of the elements participating in the intermolecular links. The notation employed in this review is meant to highlight such information because it is most valuable to the synthetic chemists



**Fig. 3.** Histograms for the distribution of intermolecular Te–D contact distances. The magnitudes are normalized to the sum of Bondi's van der Waals radii ( $\Sigma r_{vdw}$ ); the dotted line denotes the cutoff for analysis (93% of  $\Sigma r_{vdw}$ ).

who might want to explore variations on the structures of the building blocks.

### 3.2. The supramolecular synthon with a single point of attachment: [Te D]

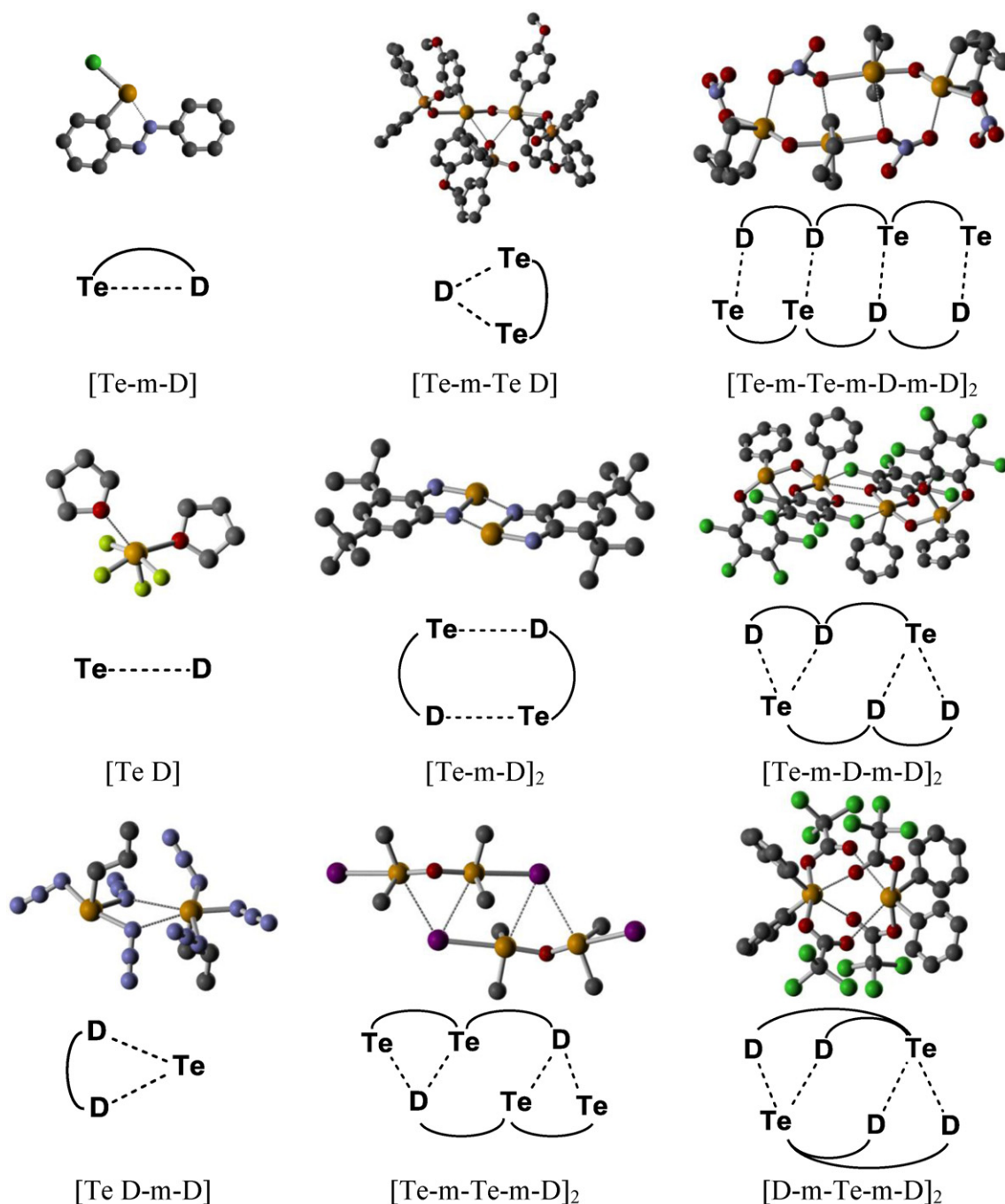
Analysis of the structures that contain the simplest supramolecular synthon helps to recognize factors that determine the characteristic geometrical features of the SBI, such as distance and angle, in the absence of other competing or supplemental interactions. [Te D] is the most abundant (50%) supramolecular synthon. Fig. 5 shows the distribution of the Te–D SBI distances in the [Te D] supramolecular synthons compared with the Te–D SBI distances in all other supramolecular synthons (Fig. 4). Table 1 summarizes the variety of three-dimensional structures which can be assembled in a crystal by strong [Te D] supramolecular synthons. The most basic structural types that are formed are 1:1 adducts with solvent molecules or ions. Examples of 1:1 adducts with pyridine or THF include the pyridine solvate of diphenylsulfiminato-trichloro-tellurium(IV) (**13**) [51] and tetrafluoro-bis(tetrahydrofuran)-tellurium (**10**) [43] while bis(triphenylphosphine)-iminium chloro-cyano-4-nitrobenzyl-tellurium(II) (**3**) [52] and bis(triphenylphosphine)-iminium bromo-cyano-4-nitrobenzyl-tellurium(II) (**4**) [52] are examples of 1:1 adducts with chloride and bromide anions, respectively. A ribbon supramolecular polymer is formed by dibromo-chlorophenyl-tellurium(IV) (**14**) [53] while a helical polymer is formed by 3,5-dimethyl-1,2-tellurazole (**12**) [54]. Examples of 2D arrays are catena-(( $\mu_2$ -chloro)-dichloro-methyl-tellurium(IV)) (**2**) [55] and catena-(4,4-bis( $\mu_2$ -chloro)-4-chloro-1-thia-3-selena-2,5-diaza-4-telluracyclopentadienyl) (**18**) [56] while a solvent capped 2D

array is formed by catena-(( $\mu_2$ -cyano)-bis(acetonitrile)-tricyano-tellurium(IV)) (**8**) [43]. The [Te D] supramolecular synthons have also been observed to direct the formation of the entire 3D lattice of a crystal, for example in the heptane solvate of dicyano-tellurium (**7**), [57] which forms a 3D lattice because its bifunctional building block forms ribbon polymers in two directions.

The distribution of X–Te–D intermolecular angles (Fig. 6) shows a marked predominance for values between  $160^\circ$  and  $180^\circ$ , although there is significant variance in the measurements. Such directional character of the SBIs is consistent with Alcock's early observations and his bonding interpretation (Fig. 1). Fig. 7 displays a histogram of SBI distances in [Te D] for the two most common coordination numbers of tellurium in the molecular building blocks (i.e. the coordination number prior to SBI formation), 2 and 4. Bearing in mind that the predominant oxidation state of Te with a coordination number of 2 is II (I in ditellurides) and that a disphenoidal tetracoordinate geometry is typical of oxidation state IV, the histogram shows no correlation between SBI distance in the [Te D] supramolecular synthon with the coordination number or oxidation state of Te.

Close inspection of the shortest SBIs ( $<80\% \Sigma r_{vdw}$ ) within the [Te D] supramolecular synthon (Table 1) reveals that they mostly involve O, N or Cl as either donor (D) or the acceptor atoms (X) in X–Te–D. The pseudohalogen group CN is also involved in these shorter interactions. Consistent with Alcock's bonding description for a SBI, as the electronegativity of X increases, the Te contribution to the Te–X  $\sigma^*$  orbital increases, facilitating overlap with the lone pair orbital of D. In addition, the energy of the acceptor orbital decreases as the Te–X bond is weakened by an increasing Te–X electronegativity difference and leads to a stronger orbital interaction





**Fig. 4.** Ball-and-stick examples and schematic representations of Te-centered SBI supramolecular synthons. Hydrogen atoms have been omitted for clarity. Original data from Refs. [40–48].

with the lone pair of D. The electrostatic component of the interaction is also enhanced by increasing the polarization of the Te–X bond.

### 3.3. Supramolecular synthons with two points of attachment

#### 3.3.1. [Te D-m-D]

There are eleven structures that contain the [Te D-m-D] supramolecular synthon with Te–D SBIs as short as 70% of the sum of  $r_{vdW}$ . This is the simplest supramolecular synthon that contains multiple points of attachment and it highlights the ability of tellurium to simultaneously form more than one SBI. Two

of these structures formed between a small molecule with two donor atoms (diglyme [58] and DME [59]) and a Te containing molecule, while five of these structures are assembled in a head to tail arrangement as Fig. 8(a). The remaining examples are a special case in which the Te atom also acts as the donor (Fig. 8(b)). Eight of the examples form an infinite 1D supramolecular polymer arranged by either motif while the remaining example is a dimer (Fig. 8(b)). Generally this synthon displays one SBI longer than the other; the notable exceptions are bis(thiobenzoato-S)-tellurium(II) (27) [60] which has two equal Te–S SBIs (88%  $\Sigma r_{vdW}$ ) and 1,1,5,5,9,9-hexachlorotelluracyclododecane dimethylformamide sesquihydrate (28) [61] which has two similar Te–Cl SBIs

**Table 1**X–Te–D SBLs for which the Te–D distance is shorter than 80% of the sum of  $r_{vdW}$  in the [Te D]<sub>2</sub> supramolecular synthon.

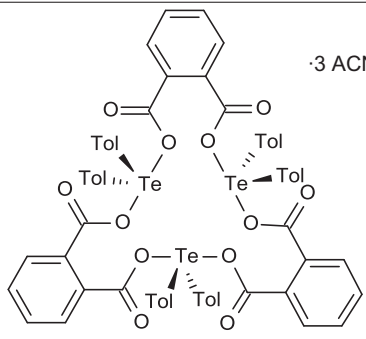
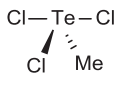
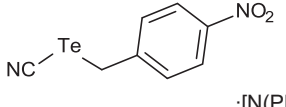
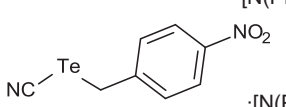
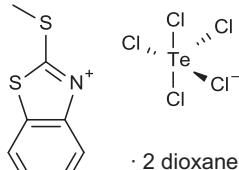
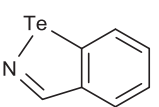
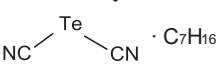
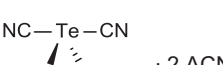
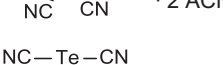

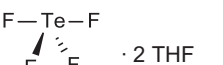

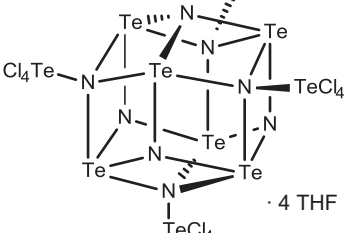
Reference	Building block	D	X	$d_{SBL}$ (Å)	% $\Sigma r_{vdW}$	$a_{SBL}$ (°)	Donor	Notes
1 [82]		N	C	2.793	77	161.9	ACN	1:1 Adduct
2 [55]		Cl	Cl	2.814	74	171.3		Polymer
3 [52]		Cl	CN	2.924	77	167.9	Cl <sup>−</sup>	1:1 Adduct
4 [52]		Br	CN	3.100	79	167.6	Br <sup>−</sup>	1:1 Adduct
5 [86]		O	Cl	2.765	77	179.7	Dioxane	1:1 Adduct
6 [67]		N	N	2.456	68	165		Helical polymer
7 [57]		N	N	2.465	68	165.7		
		N	N	2.488	69	166.7		
		N	CN	2.745	76	163.2		3D network
8 [43]		N	CN	2.758	76	163.9		
		N	CN	2.601	72	158.5		2D network
9 [43]		N	CN	2.727	76	145.0	ACN	1:1 Adduct
		N	CN	2.866	79	136.1	ACN	1:1 Adduct
		N	CN	2.567	71	148.9		Polymer
		O	CN	2.701	75	147.1	THF	1:1 Adduct
		O	CN	2.715	76	138.8	THF	1:1 Adduct
		O	CN	2.774	77	140.7	THF	1:1 Adduct
10 [43]		O	F	2.448	68	138.8	THF	1:1 Adduct
11 [87]		O	F	2.696	75	140.7	THF	1:1 Adduct
		O	N	2.695	75	172.6	THF	1:1 Adduct
12 [54]		O	N	2.715	76	172.6	THF	1:1 Adduct
		O	N	2.717	76	172.2	THF	1:1 Adduct
		O	N	2.726	76	172.8	THF	1:1 Adduct
		N	N	2.640	73	167.4		Helical polymer
		N	N	2.659	74	168.3		
		N	N	2.700	75	166.4		
		N	N	2.741	76	168.9		
		N	N	2.744	76	167.0		
		N	N	2.774	77	173.3		

Table 1 (Continued)

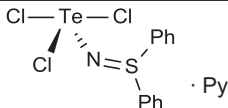
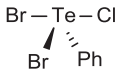
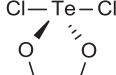
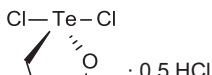
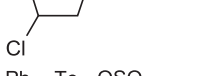
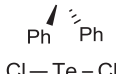
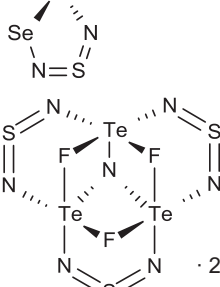
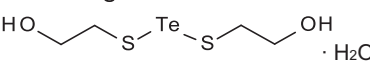
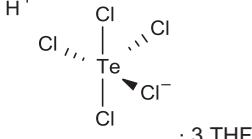
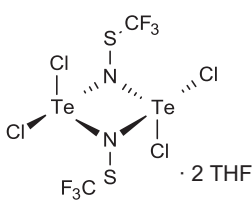
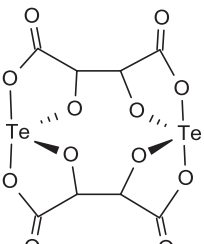
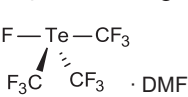
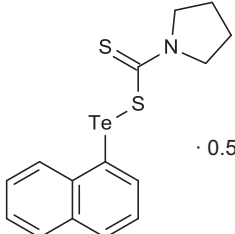
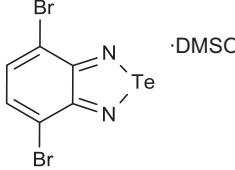
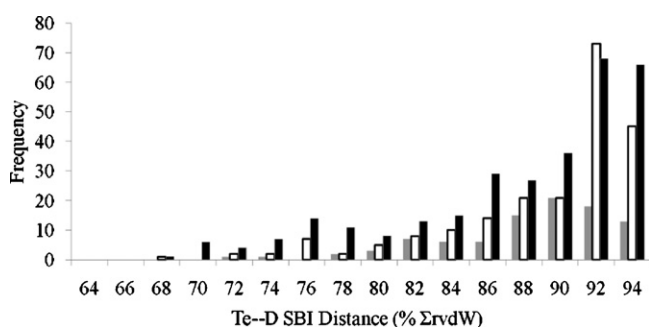
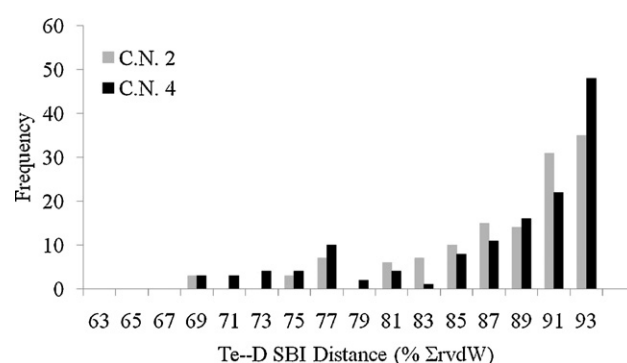
	Reference	Building block	D	X	$d_{\text{SBI}}$ (Å)	% $\Sigma r_{\text{vdW}}$	$a_{\text{SBI}}$ (°)	Donor	Notes
13	[51]	 · Py	N	Cl	2.426	67	177.5	Py	1:1 Adduct
14	[53]		Cl	Br	2.811	74	175.0		Polymer
15	[88]	 · NH <sub>4</sub> Cl	Cl	O	2.723	71	159	Cl <sup>−</sup>	1:1 Adduct
16	[89]	 · 0.5 HCl	Cl	O	2.918	77	168.4		Dimer
17	[90]	 · 5 H <sub>2</sub> O	O	C	2.797	78	173.2	H <sub>2</sub> O	1:1 Adduct
18	[56]		Cl	N	2.933	77	159.7		Polymer
19	[91]	 · 2 Py	N	N	2.677	74	162.4	Py	1:1 Adduct
20	[92]	 · H <sub>2</sub> O	N O O	N S S	2.852 2.495 2.666	79 70 74	155.4 133.0 134.4	Py H <sub>2</sub> O H <sub>2</sub> O	1:1 Adduct 1:1 Adduct 1:1 Adduct
21	[24]	 · 3 THF	O	Cl	2.593	72	180.0	THF	1:1 Adduct
22	[93]	 · 2 THF	O	Cl	2.448	68	177.9	THF	1:1 Adduct
23	[94]	 · 4 DMSO	O O O O	O O O O	2.550 2.572 2.696 2.796	71 72 75 78	165.3 164.6 168.5 168.68	DMSO DMSO DMSO DMSO	4:1 adduct 4:1 Adduct 4:1 Adduct 4:1 Adduct
24	[95]	 · DMF	F	C	2.566	73	167.16		Polymer

Table 1 (Continued)

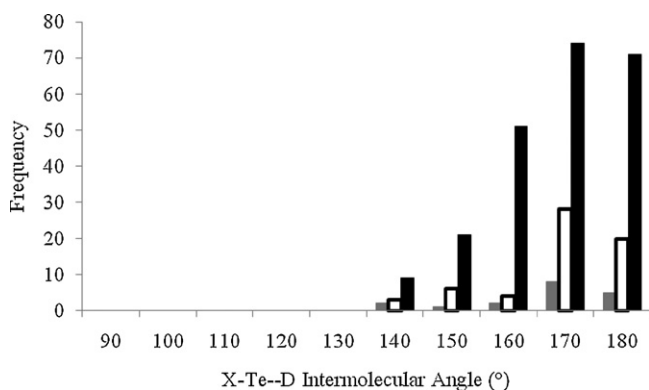
	Reference	Building block	D	X	$d_{\text{SBI}}$ (Å)	$\% \Sigma r_{\text{vdW}}$	$a_{\text{SBI}}$ (°)	Donor	Notes
			O	C	2.702	75	169.5	DMF	1:1 Adduct
25	[96]	 · 0.5 CH <sub>2</sub> Cl <sub>2</sub>	S	S	3.042	79	167.23		Dimer
26	[66]	 · DMSO	O	N	2.834	79.2	163.0	DMSO	1:1 Adduct



**Fig. 5.** Histogram for the distribution of Te–D interaction distances in [Te D] (■), [Te–m–D]<sub>2</sub> (□) and all other supramolecular synthons (■).

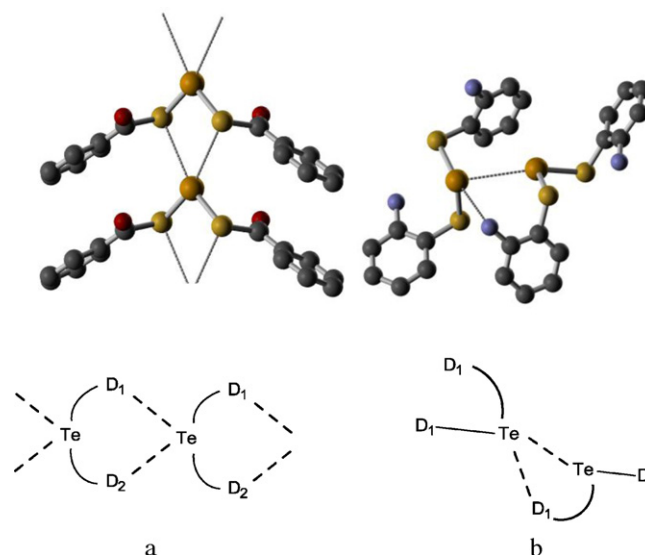
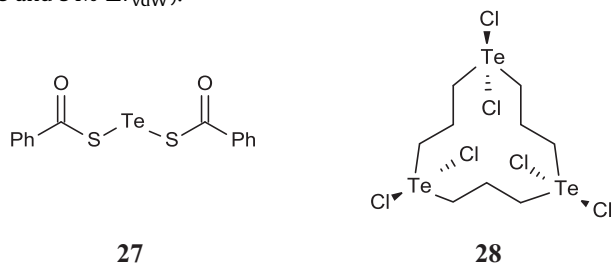


**Fig. 7.** Distribution of SBI distances in the [Te D] supramolecular synthon for tellurium building blocks with coordination numbers 2 and 4.



**Fig. 6.** Histogram for the distribution of X–Te–D intermolecular angles in [Te D]. Data are classified by the magnitude of the SBI distance as a fraction of the sum of van de Waals radii: 64–73% (■), 74–83% (□) and 84–93% (■).

(88 and 91%  $\Sigma r_{\text{vdW}}$ ).



**Fig. 8.** Ball and stick representations of the arrangement of (a) polymer formed by bis(thiobenzoato-S)-tellurium(II) [60], and the (b) bis(2-aminobenzenethiolato)-tellurium dimer [62].

### 3.3.2. [Te–m–Te D]

Six crystal structures contain the [Te–m–Te D] supramolecular synthon with Te–D SBIs as short as 82% of the sum of  $r_{\text{vdW}}$ . Three of the examples display the [Te–m–Te D] supramolecular synthon cap-



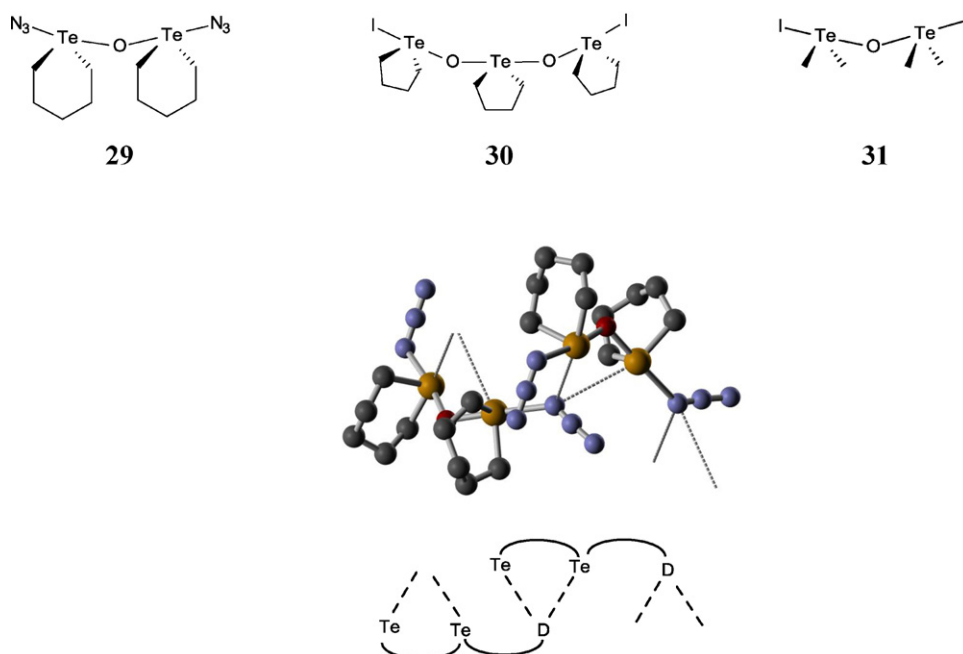


Fig. 9. Ball and stick representation of the arrangement of molecules in the crystal [63] of **29**. H atoms have been removed for clarity.

ping open tellurium sites limiting the supramolecular structure to monomers or dimers. Compounds  $(\mu_2\text{-oxo})\text{-bis}(\text{azido})\text{-(pentane-1,5-diyl)-di-tellurium(IV)}$  (**29**) [63] and  $\text{bis}(\mu_2\text{-oxo})\text{-di-iodo-tris(butane-1,4-diyl)-tri-tellurium(IV)}$  (**30**) [47] associate to form supramolecular ribbon polymer structures (Fig. 9) through  $[\text{Te}-1\text{-Te N}]_2$  and  $[\text{Te}-1\text{-Te I}]_2$  respectively, while  $(\mu_2\text{-oxo})\text{-di-iodo-tetramethyl-di-tellurium(IV)}$  (**31**) [47] forms a 2D network through  $[\text{Te}-1\text{-Te I}]_2$  supramolecular synthons.

### 3.3.3. $[\text{Te}-m-\text{D}]_2$

After the  $[\text{Te D}]$  supramolecular synthon  $[\text{Te}-m-\text{D}]_2$  is the second most common, totaling 41% of the analyzed structures. As in the case of  $[\text{Te D}-m-\text{D}]$  and  $[\text{Te}-m-\text{Te D}]$ , there are two points of attachment, but each D and Te atom make a single SBI for each synthon. The  $[\text{Te}-m-\text{D}]_2$  supramolecular synthons are virtual heterocycles with two antiparallel SBIs. While  $m$  ranges from 0 to 6 (4–16-membered virtual rings), its most common value is 0 (as in 131 of 172 structures). While  $[\text{Te}-m-\text{D}]_2$  has a distribution of distances similar to that of  $[\text{Te D}]$  (Fig. 5), it is in principle stronger as there are twice as many supramolecular interactions per synthon. As observed for  $[\text{Te D}]$ , the shortest SBIs are formed when N or O donate electrons into  $\text{Te}-\text{X}$  bonds and X is also N or O. Within this set, there are fifteen structures with  $\text{Te}-\text{D}$  SBIs shorter than 80% of the sum of  $r_{\text{vdW}}$  (Table 2) and in each case the actual supramolecular synthon is the virtual four-membered heterocycle  $[\text{Te}-\text{D}]_2$ . Six of these crystal structures (1,2,5-telluradiazole (**32**) [64], phenanthro(9,10-c)-1,2,5-telluradiazole (**33**) [65], 4,6-di-*t*-butylbenzo-2,1,3-telluradiazole (**37**) [44], benzo-2,1,3-telluradiazole (**38**) [66], 4,7-dibromobenzo-2,1,3-telluradiazole (**39**) [66], and the DMSO adduct of 4,7-dibromobenzo-2,1,3-telluradiazole (**26**) [66]) feature the synthon  $[\text{Te}-\text{N}]_2$  assembled by 1,2,5-telluradiazole heterocyclic building blocks. The corresponding SBIs are very short; the same is observed for the SBIs in  $[\text{Te D}]$  (Table 1) formed by 1,2-tellurazole heterocycles, **6** [67] and **12** [54]. Interestingly, the shortest  $\text{Te}-\text{N}$  SBIs are observed in  $[\text{Te}-\text{N}]_2$  between two cationic heterocycles: **40**, **41**, and **42** [68,69]. Of all tellurium-based supramolecular synthons,  $[\text{Te}-\text{N}]_2$  has been studied in the greatest detail. Its binding energy has been calculated in several systems. HF/3-21+G(d,p) [70] gave  $-43.84$  kJ/mol

in the case of bis(dimethylamino)-tellurium(II) (**43**) [71]. Values obtained with relativistic GGA DFT (PW91/TZP, ZORA) range from  $-54$  kJ/mol [72] to  $-72$  kJ/mol, [66] for 1,2,5-telluradiazole (**32**) and its annulated derivatives. Hybrid DFT (B3LYP/6-31G(d,p), SDB-cc-pVTZ for Te) showed that the dimers of the cations **40** and **41** are minima in the potential energy surface but the overall intermolecular interactions would be repulsive in gas phase; favourable binding energies are obtained only after inclusion of the dielectric properties of the medium (acetonitrile) modeled by the Polarized Continuum Model:  $-53.5$  for **40** and  $-22$  kJ/mol for **41** [68,69]. Meticulous DFT mapping of the potential energy surface by distortion of the  $[\text{Te}-\text{N}]_2$  supramolecular synthon [15] has been used to parameterize a force field for the design of new supramolecular assemblies [73]. Steric effects on the formation of the synthon have also been examined [66]. In addition to the strength of the  $\text{Te}-\text{N}$  SBIs, telluradiazoles have received much attention because of their convenient synthesis as well as the many applications of their lighter analogues, including in electronic materials [74–76]. Recently, the chromotropism of two polymorphs of 4,5,6,7-tetrafluorobenzo-2,1,3-telluradiazole [77] was explained in terms of changes of the local symmetry of distorted  $[\text{Te}-\text{N}]_2$  synthons. Also, noncentrosymmetric distortion of the supramolecular synthon was used to induce the crystallization of noncentrosymmetric lattices with nonlinear optical properties [78].

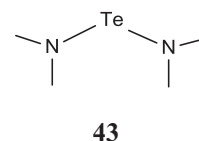
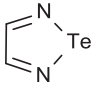
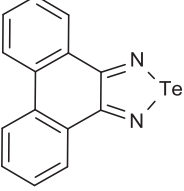
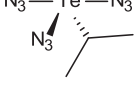
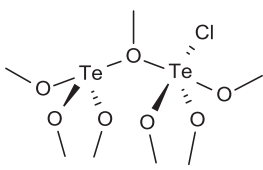
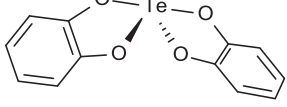
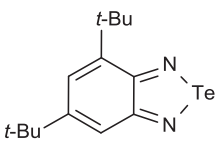
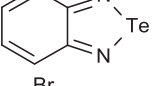
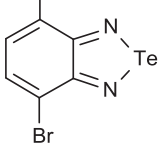
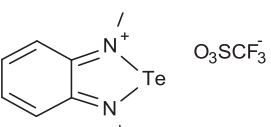
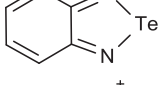
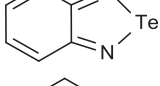
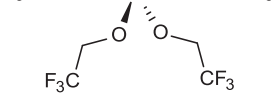
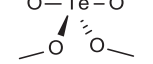
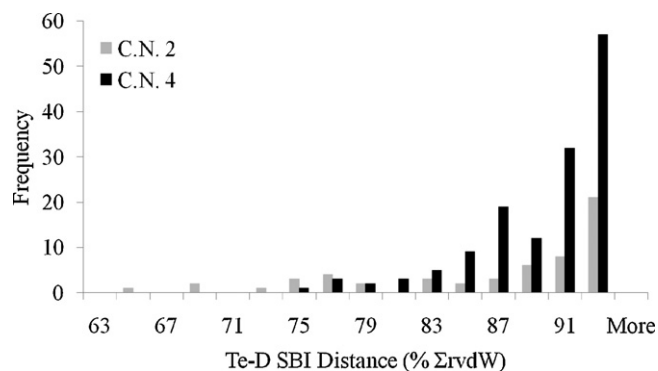


Fig. 10 shows the histograms of SBI distances for the  $[\text{Te}-m-\text{D}]_2$  supramolecular synthon classified according to the coordination number of tellurium in the molecular building block. In spite of the smaller number of examples, it is apparent that in these synthons two-coordinate Te participates in shorter SBIs than tetra-coordinate tellurium. This observation is in contrast with the case of  $[\text{Te D}]$ , in which the distribution of distances for one and the other coordination numbers follows the same trend. The difference can be attributed to the different steric demands of dimerization at

**Table 2**X–Te–D SBIs for which the Te–D distance is shorter than 80% of the sum of  $r_{\text{vdW}}$  in the [Te–*m*–D]<sub>2</sub> supramolecular synthon.

	Reference	Building block	D	X	$d_{\text{SBI}}$ (Å)	% $\Sigma r_{\text{vdW}}$	$\alpha_{\text{SBI}}$ (°)	Notes
32	[64]		N	N	2.764	77	151.9	Polymer
33	[65]		N N	N N	2.825 2.842	78 79	150.9 151.2	Polymer
34	[46]		N	N	2.852	79	146.7	Dimer
15	[88]		O	O	2.764	77	145.4	Dimer
35	[97]		O	O	2.692	75	171.4	Dimer
36	[98]		O	O	2.644	74	153.7	Polymer
			O	O	3.285	92	138.4	
37	[44]		N	N	2.629	73	155.7	Dimer
38	[66]		N N N N	N N N N	2.682 2.688 2.714 2.720	74 74 75 75	153.3 153.5 152.4 152.6	Polymer Polymer Polymer Polymer
39	[66]		N	N	2.696	74	156.2	Dimer
26	[66]		N	N	2.743	76	155.3	Dimer
40	[68]		N	N	2.417	67	150.0	Dimer
41	[69]		N	S	2.537	70	154.3	Dimer
42	[69]		N	S	2.553	71	155.7	Dimer
44	[99]		O	O	2.804	78	160.8	Dimer
45	[99]		O O	O O	2.815 2.88	79 80	162.0 162.0	Polymer Polymer



**Fig. 10.** Distribution of SBI distances in the  $[\text{Te}-m-\text{D}]_2$  supramolecular synthon for tellurium building blocks with coordination numbers 2 and 4.

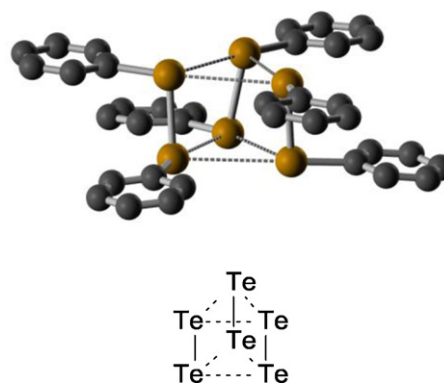
the Te(IV) and Te(II) centers. Another contributing factor would be related to Bent's rule, according to which "atomic *s*-character concentrates in orbitals directed toward electropositive substituents" [79]. The most electronegative substituents in a Te(IV) disphenoidal center therefore, prefer to occupy the axial position where they cannot facilitate the formation of a short Te–D SBI.

The variety of supramolecular structures constructed by the  $[\text{Te}-m-\text{D}]_2$  supramolecular synthons are in principle more limited than those observed with  $[\text{Te}-\text{D}]$  due to a reduction in the number of degrees of freedom. The  $[\text{Te}-m-\text{D}]_2$  supramolecular synthon leads predominantly to isolated dimers or 1D ribbon polymers. The 1D polymers can be divided into two categories illustrated in Fig. 11, those in which a single tellurium center is part of two supramolecular synthons and those where two tellurium atoms are necessary for the formation of two supramolecular synthons. The latter case is more closely related to that of discrete dimers. Another interesting example is the cyclic trimer constructed by bis(pentafluorophenyl)-di-tellurium(I) (**46**) that forms a virtual 6-membered triangular prism with the  $[\text{Te}-\text{D}]_3$  supramolecular synthon (Fig. 12) [80].

### 3.4. Supramolecular synthons with four points of attachment

#### 3.4.1. $[\text{Te}-m-\text{Te}-m-\text{D}]_2$

This supramolecular synthon can also be regarded as two  $[\text{Te}-m-\text{Te}-\text{D}]$  supramolecular synthons working cooperatively or a  $[\text{Te}-m-\text{D}]_2$  supramolecular synthon with two additional SBIs. There are ten examples of the  $[\text{Te}-m-\text{Te}-m-\text{D}]_2$  supramolecular synthon, and these lead to isolated dimers, ribbon polymers or 2D networks,

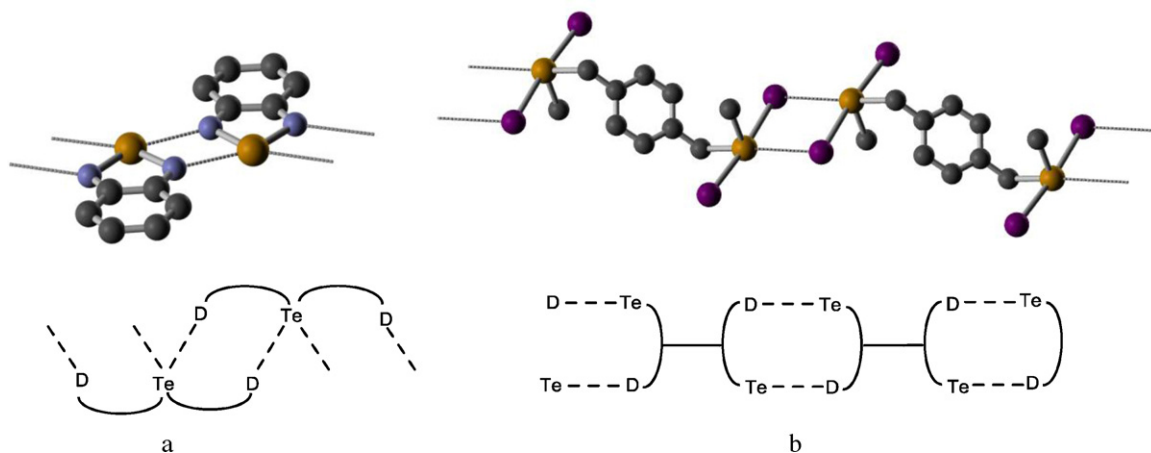
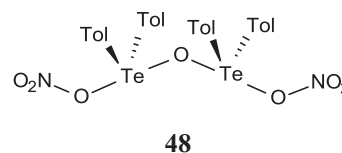


**Fig. 12.** Ball and stick representation of the arrangement of molecules of bis(pentafluorophenyl) ditelluride, **46**, in the crystal lattice [80]. F atoms are removed for clarity.

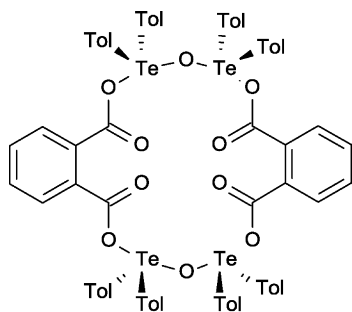
some in conjunction with  $[\text{Te}-m-\text{Te}-m-\text{D}-m-\text{D}]_2$ . The shortest Te–D SBI distance (C–Te–O) is 82% of the sum of  $r_{vdW}$  and is found in the  $[\text{Te}-1-\text{Te}-5-\text{O}]_2$  supramolecular synthon between bis(( $\mu_2$ -phthalato- $\text{O},\text{O}'$ )-(  $\mu_2$ -oxo)-tetrakis(p-tolyl)-di-tellurium) p-xylene solvate (**47**) [82]. Nine of the molecules which associate to form  $[\text{Te}-m-\text{Te}-m-\text{D}]_2$  have a  $\mu_2$ -oxo bridged bistellurium(IV) motif (Scheme 2) in their building block.

#### 3.4.2. $[\text{Te}-m-\text{Te}-m-\text{D}-m-\text{D}]_2$

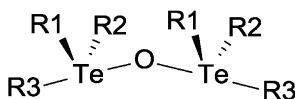
This supramolecular synthon is present in six crystal structures with the shortest Te–D SBI distance (C–Te–O) at 78% of the sum of  $r_{vdW}$  between ( $\mu_2$ -oxo)-bis(butane-1,4-diyl)-(dinitrato- $\text{O}$ )-di-tellurium (**48**) in  $[\text{Te}-1-\text{Te}-2-\text{O}-1-\text{O}]_2$  [42]. Five of the crystals contain a  $\mu_2$ -oxo bridged bistellurium(IV) motif (Scheme 2) within their building block. Three of these structures participate in the  $[\text{Te}-1-\text{Te}-2-\text{O}-1-\text{O}]_2$  supramolecular synthon while the other two participate in  $[\text{Te}-1-\text{Te}-2-\text{O}-4-\text{O}]_2$  or  $[\text{Te}-3-\text{Te}-\text{O}-3-\text{O}]_2$ .  $[\text{Te}-m-\text{Te}-m-\text{D}-m-\text{D}]_2$  can be viewed as a  $[\text{Te}-m-\text{D}]_2$  supramolecular synthon with two peripheral  $[\text{Te}-\text{D}]$  supramolecular synthons. In the known structures this supramolecular synthons generates either dimers or ribbon polymers.



**Fig. 11.** Ball and stick representations of the arrangement of molecules in the lattices of (a) **38** [54] and (b) ( $\mu_2$ -p-xylene)-tetraiodo-dimethyl-di-tellurium(IV) [81]. H atoms are removed for clarity.



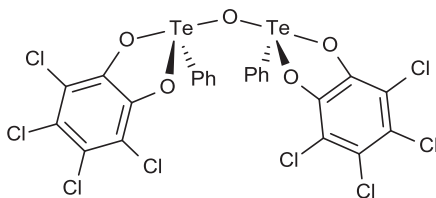
47



**Scheme 2.** ( $R_1$ ,  $R_2$  = aryl, alkyl,  $R_3$  = aryl,  $\text{NO}_3$ ) [42,47,83,84].

### 3.4.3. $[\text{Te}-m-D-m-D]_2$ or $[D-m-\text{Te}-m-D]_2$

This motif arises from a  $[\text{Te}-D]_2$  supramolecular synthon with two additional peripheral SBIs or two  $[\text{Te } D-m-D]$  supramolecular synthons. It is observed in four crystal structures, three of which contain the  $[D-m-\text{Te}-m-D]_2$  supramolecular synthon. In the known structures these supramolecular synthons only form dimers. The shortest Te–O SBI distance, 83% of the sum of  $r_{\text{vdW}}$ , are observed in ( $\mu_2$ -oxo)-bis((tetrachlorocatecholato- $O,O'$ )-phenyl-tellurium(IV)) tetrahydrofuran solvate (**49**) in the  $[\text{Te}-O-2-\text{Cl}]_2$  supramolecular synthon [45].



49

## 4. Conclusions

This survey of the structures of tellurium compounds provides compelling evidence of the influence that SBIs centered on the chalcogen have on supramolecular organization in the solid state. A significant proportion of the known structures of tellurium compounds do display short intermolecular contacts centered on the chalcogen, all of them fall within one of eight different tellurium-centered supramolecular synthons that contain one to four Te–D SBIs. The shortest—and likely strongest—tellurium SBIs are formed with oxygen, nitrogen or chlorine atoms; on the other hand the interaction is also strengthened by the attachment of tellurium to the same strongly electron-withdrawing elements and the CN group. Supramolecular synthons with more points of attachment are expected to be stronger and indeed can afford shorter SBIs, provided that steric repulsion is not important. Two types of molecular building blocks appear to be convenient for the design and construction of supramolecular structures. Molecules containing the 1,2,5-telluradiazole ring, which associate forming the  $[\text{Te}-N]_2$  supramolecular synthon, are already being applied in crystal engi-

neering of functional materials. Although less investigated,  $\mu_2$ -oxo bridged bis-Te(IV) compounds are specially interesting because of their ability to form synthons with four points of attachment. Aside from 1:1 adducts with solvents or anions, there is a conspicuous absence of heteromolecular association. Complementary pairs, capable of molecular recognition through supramolecular synthons with multiple SBIs, would eventually provide a new platform for programmable self-assembly [85]; it is one of the most promising lines of future research. Paraphrasing Gleiter et al. [23], there is a *world beyond hydrogen bonds* waiting to be explored, but realizing its potential still requires an important amount of fundamental research.

## References

- [1] M. Nic, J. Jirat, B. Kosata, A. Jenkins, in: A.D. McNaught, A. Wilkinson (Eds.), The "Gold Book", 2nd ed., Blackwell Scientific Publications, Oxford, 1997.
- [2] R.J. Puddephatt, *Coord. Chem. Rev.* 216–217 (2001) 313.
- [3] P. Pyykko, *Chem. Rev.* 97 (1997) 597.
- [4] I. Haiduc, in: J. Steed, J. Atwood (Eds.), *Encyclopedia of Supramolecular Chemistry*, Marcel Dekker, Inc., New York, 2004, p. 1215.
- [5] W.-W.d. Mont, A.M.-v. Salzen, F. Ruthe, E. Seppälä, G. Muges, F.A. Devillanova, V. Lippolis, N. Kuhn, *J. Organomet. Chem.* 623 (2001) 14.
- [6] C. Bleiholder, D.B. Werz, H. Koppel, R. Gleiter, *J. Am. Chem. Soc.* 128 (2006) 2666.
- [7] A. Mohajeri, A.H. Pakiari, N. Bagheri, *Chem. Phys. Lett.* 467 (2009) 393.
- [8] M.G. Newton, R.B. King, I. Haiduc, A. Silvestru, *Inorg. Chem.* 32 (1993) 3795.
- [9] T. Clark, M. Hennemann, J. Murray, P. Politzer, *J. Mol. Model.* 13 (2007) 291.
- [10] J.-M. Chen, B.K. Santra, C.W. Liu, *Inorg. Chem. Commun.* 7 (2004) 1103.
- [11] I. Vargas-Baca, T. Chivers, *Phosphorus Sulfur Silicon Relat. Elem.* 164 (2000) 207.
- [12] T. Chivers, *A Guide To Chalcogen-Nitrogen Chemistry*, World Scientific Publishing, Hackensack, NJ, 2006.
- [13] P.H. Svensson, L. Kloo, *Chem. Rev.* 103 (2003) 1649.
- [14] N.W. Alcock, *Adv. Inorg. Chem. Radiochem.* 15 (1972) 1.
- [15] A.F. Cozzolino, I. Vargas-Baca, S. Mansour, A.H. Mahmoudkhani, *J. Am. Chem. Soc.* 127 (2005) 3184.
- [16] T. Chivers, I. Krouse, M. Parvez, I. Vargas-Baca, T. Ziegler, P. Zoricak, *Inorg. Chem.* 35 (1996) 5836.
- [17] P. Politzer, J.S. Murray, P. Lane, *Int. J. Quantum Chem.* 107 (2007) 3046.
- [18] J.N. Israelachvili, *Intermolecular and Surface Forces*, Academic, London, 1985, p. 83.
- [19] J.W. Steed, J.L. Atwood, *Supramolecular Chemistry*, Wiley, New York, 2000.
- [20] J. Starbuck, N.C. Norman, A.G. Orpen, *New J. Chem.* 23 (1999) 969.
- [21] S.C. James, N.C. Norman, A.G. Orpen, J. Starbuck, *CrystEngComm* 2 (2000) 67.
- [22] I. Haiduc, J. Zukerman-Schpector, *Phosphorus Sulfur Silicon Relat. Elem.* 171 (2001) 171.
- [23] R. Gleiter, D.B. Werz, B.J. Rausch, *Chem. Eur. J.* 9 (2003) 2676.
- [24] D.B. Werz, R. Gleiter, F. Rominger, *J. Am. Chem. Soc.* 124 (2002) 10638.
- [25] D.B. Werz, T.H. Staeb, C. Benisch, B.J. Rausch, F. Rominger, R. Gleiter, *Org. Lett.* 4 (2002) 339.
- [26] J.A.R.P. Sarma, F.H. Allen, V.J. Hoy, J.A.K. Howard, R. Thaimattam, K. Biradha, G.R. Desiraju, *Chem. Commun.* (1997) 101.
- [27] A. Farina, M. Stefano Valdo, M. Maria Teresa, M. Pierangelo, R. Giuseppe, V. Giuseppe, *Angew. Chem., Int. Ed.* 38 (1999) 2433.
- [28] P. Metrangolo, Y. Carcenac, M. Lahtinen, T. Pilati, K. Rissanen, A. Vij, G. Resnati, *Science* 323 (2009) 1461.
- [29] J. Clemente-Juan, E. Coronado, G. Minguez Espallargas, H. Adams, L. Brammer, *CrystEngComm* 12 (2010) 2339.
- [30] G.R. Desiraju, *Angew. Chem., Int. Ed.* 34 (1995) 2311.
- [31] R.P. Sijbesma, F.H. Beijer, L. Brunsveld, B.J.B. Folmer, J.H.K.K. Hirschberg, R.F.M. Lange, J.K.L. Lowe, E.W. Meijer, *Science* 278 (1997) 1601.
- [32] N.N. Greenwood, A. Earnshaw, *Chemistry of the Elements*, 2nd ed., Butterworth-Heinemann, Oxford, Boston, 1998.
- [33] W.C. Cooper, *Tellurium*, Van Nostrand Reinhold Co., New York, 1971.
- [34] J. Zukerman-Schpector, I. Haiduc, *CrystEngComm* 4 (2002) 178.
- [35] F.H. Allen, *Acta Cryst. B* 58 (2002) 380.
- [36] A. Bondi, *J. Phys. Chem.* 68 (1964) 441.
- [37] R.S. Rowland, R. Taylor, *J. Phys. Chem.* 100 (1996) 7384.
- [38] I. Dance, *New J. Chem.* 27 (2003) 22.
- [39] N. Sudha, H.B. Singh, *Coord. Chem. Rev.* (1994) 469.
- [40] Z. Majeed, W.R. McWhinnie, T.A. Hamor, *J. Organomet. Chem.* 549 (1997) 257.
- [41] J. Beckmann, D. Dakternieks, A. Duthie, N.A. Lewcenko, C. Mitchell, M. Schurmann, *Z. Anorg. Allg. Chem.* 631 (2005) 1856.
- [42] H.W. Roesky, R.J. Butcher, S. Bajpai, P.C. Srivastava, *Phosphorus, Sulfur Silicon Relat. Elem.* 161 (2000) 135.
- [43] D. Lentz, M. Szwak, *Angew. Chem., Int. Ed.* 44 (2005) 5079.
- [44] T. Chivers, X. Gao, M. Parvez, *Inorg. Chem.* 35 (1996) 9.
- [45] Z. Tian, D.G. Tuck, *J. Organomet. Chem.* 462 (1993) 125.
- [46] T.M. Klapotke, B. Krumm, P. Mayer, H. Piotrowski, O.P. Ruscitti, A. Schiller, *Inorg. Chem.* 41 (2002) 1184.

- [47] J. Beckmann, J. Bolsinger, J. Spandl, *J. Organomet. Chem.* 693 (2008) 957.
- [48] N.W. Alcock, J. Culver, S.M. Roe, *J. Chem. Soc., Dalton Trans.* (1992) 1477.
- [49] J. Bernstein, R.E. Davis, L. Shimoni, N.-L. Chang, *Angew. Chem., Int. Ed.* 34 (1995) 1555.
- [50] M.C. Etter, J.C. MacDonald, J. Bernstein, *Acta Cryst. B* 46 (1990) 256.
- [51] J. Munzenberg, H.W. Roesky, M. Noltemeyer, S. Besser, R. Herbst-Irmer, *Z. Naturforsch., B: Chem. Sci.* 48 (1993) 199.
- [52] K. Maartmann-Moe, J. Songstad, *Acta Chem. Scand. A* 36 (1982) 829.
- [53] D. Rainville, R.A. Clingaro, E.A. Meyers, *Cryst. Struct. Commun.* 9 (1980) 77.
- [54] G.D. Munno, F. Lucchesini, *Acta Cryst. C* 48 (1992) 1437.
- [55] J. Pietikainen, R.S. Laitinen, J. Konu, J. Valkonen, *Z. Naturforsch., B* 56 (2001) 1369.
- [56] A. Haas, J. Kasprowski, M. Pryka, *Chem. Ber.* 125 (1992) 789.
- [57] T.M. Klapotke, B. Krumm, J.C.G. Ruiz, H. Noth, I. Schwab, *Eur. J. Inorg. Chem.* (2004) 4764.
- [58] D. Lentz, M. Szwak, *Dalton Trans.* (2008) 1289.
- [59] S. Fritz, D. Lentz, M. Szwak, *Eur. J. Inorg. Chem.* (2008) 4683.
- [60] I. Subrahmanyam, G. Aravamudan, G.C. Rout, M. Seshasayee, *J. Crystallogr. Spectrosc. Res.* 14 (1984) 239.
- [61] R.E. Marsh, *Acta Cryst. B* 61 (2005) 359.
- [62] H. Fleischer, D. Schollmeyer, *Inorg. Chem.* 41 (2002) 4739.
- [63] T.M. Klapotke, B. Krumm, P. Mayer, M. Scherr, *Z. Naturforsch., B* 61 (2006) 528.
- [64] V. Bertini, P. Dapporto, F. Lucchesini, A. Segà, A.D. Munno, *Acta Cryst. C* 40 (1984) 653.
- [65] R. Neidlein, D. Knecht, A. Gieren, C. Ruiz-Perez, *Z. Naturforsch., B* 42 (1987) 84.
- [66] A.F. Cozzolino, J.F. Britten, I. Vargas-Baca, *Cryst. Growth Design* 6 (2006) 181.
- [67] H. Campsteyn, L. Dupont, J. Lamotte-Brasseur, M. Vermeire, *J. Heterocycl. Chem.* 15 (1979) 745.
- [68] M. Risto, R.W. Reed, C.M. Robertson, R. Oilunkaniemi, R.S. Laitinen, R.T. Oakley, *Chem. Commun. (Cambridge, UK)* (2008) 3278.
- [69] M. Risto, A. Assoud, S.M. Winter, R. Oilunkaniemi, R.S. Laitinen, R.T. Oakley, *Inorg. Chem.* 47 (2008) 10100.
- [70] C. Kontopoulos, M.P. Sigalas, *J. Mol. Struct.: THEOCHEM* 490 (1999) 125.
- [71] R.E. Allan, H. Gornitzka, J. Karcher, M.A. Paver, M.-A. Rennie, C.A. Russell, P.R. Raithby, D. Stalke, A. Steiner, D.S. Wright, *J. Chem. Soc., Dalton Trans.* (1996) 1727.
- [72] A.F. Cozzolino, I. Vargas-Baca, S. Mansour, A.H. Mahmoudkhani, *J. Am. Chem. Soc.* 40 (2005) 4966.
- [73] A.F. Cozzolino, I. Vargas-Baca, *Cryst. Growth Des.* 11 (2011), doi:10.1021/cg100951y.
- [74] J. Huan, Y. Niu, Y. Xu, Q. Hou, W. Yan, Y. Mo, M. Yua, Y. Cao, *Synth. Met.* 135–136 (2003) 181.
- [75] J.P. Kochansky, C.F. Cohen, W.R. Lusby, J.A. Svoboda, J. Feldmesser, F.C. Wright, *J. Ag. Entomol.* 5 (1988) 131.
- [76] B.A.D. Neto, A.S.A. Lopes, G. Ebeling, R.S. Gonçalves, V.E.U. Costa, F.H. Quina, J. Dupont, *Tetrahedron* 61 (2005) 10975.
- [77] A.F. Cozzolino, P.S. Whitfield, I. Vargas-Baca, *J. Am. Chem. Soc.* 132 (2010) 17265.
- [78] A.F. Cozzolino, Q. Yang, I. Vargas-Baca, *Cryst. Growth Des.* 10 (2010) 4959.
- [79] H.A. Bent, *Chem. Rev.* 61 (1961) 275.
- [80] T.M. Klapotke, B. Krumm, P. Mayer, K. Polborn, O.P. Ruscitti, *J. Fluorine Chem.* 112 (2001) 207.
- [81] M.J. Hesford, N.J. Hill, W. Levason, G. Reid, *J. Organomet. Chem.* 689 (2004) 1006.
- [82] K. Kobayashi, H. Izawa, K. Yamaguchi, E. Horn, N. Furukawa, *Chem. Commun.* (2001) 1428.
- [83] M.M. Mangion, M.R. Smith, E.A. Meyers, *J. Heterocycl. Chem.* 10 (1973) 543.
- [84] N.W. Alcock, W.D. Harrison, *J. Chem. Soc., Dalton Tans.* (1982) 1421.
- [85] F.A. Aldaye, A.L. Palmer, H.F. Sleiman, *Science* 321 (2008) 1795.
- [86] W. Hinrichs, D. Mandak, G. Klar, *Cryst. Struct. Commun.* 11 (1982) 1781.
- [87] W. Massa, C. Lau, M. Möhlen, B. Neumüller, K. Dehnicke, *Angew. Chem., Int. Ed.* 37 (1998) 2840.
- [88] M.R. Sundberg, R. Uggla, T. Laitalainen, J. Bergman, *J. Chem. Soc., Dalton Trans.* (1994) 3279.
- [89] H. Fleischer, B. Mathiasch, D. Schollmeyer, *Organometallics* 21 (2002) 526.
- [90] M.J. Collins, J.A. Ripmeester, J.F. Sawyer, *J. Am. Chem. Soc.* 110 (1988) 8583.
- [91] J. Munzenberg, H.W. Roesky, S. Besser, R. Herbst-Irmer, G.M. Sheldrick, *Inorg. Chem.* 31 (1992) 2986.
- [92] H. Fleischer, D. Schollmeyer, *Angew. Chem., Int. Ed.* 39 (2000) 3705.
- [93] R. Boese, J. Dworak, A. Haas, M. Pryka, *Chem. Ber.* 128 (1995) 477.
- [94] S. Yosef, M. Brodsky, B. Sredni, A. Albeck, M. Albeck, *ChemMedChem* 2 (2007) 1601.
- [95] N.V. Kirij, Y.L. Yagupolskii, W. Tyrre, I. Pantenburg, D. Naumann, Z. Anorg. Allg. Chem. 633 (2007) 943.
- [96] M.D. Rudd, A. Defferding, K. Klausmeyer, *Phosphorus, Sulfur Silicon Relat. Elem.* 183 (2008) 2361.
- [97] H. Fleischer, D. Schollmeyer, *Inorg. Chem.* 40 (2001) 324.
- [98] O. Lindqvist, *Acta Chem. Scand.* 21 (1967) 1473.
- [99] R. Betz, M. Stapel, M. Pfister, F.W. Roessner, M.M. Reichvilser, P. Klufers, Z. Anorg. Allg. Chem. 634 (2008) 2391.